PaperID **AU184**

Author **D P Dinesh Babu , Oil India Limited , India**

Co-Authors **Das Pradipta Kumar, Nirmal Kundu, Sujata Rani Mishra**

Predicting the distribution of volcanics by geocellular modeling approach: a case study from Onland and Shallow Offshore Mahanadi Basin, India

Abstract

Mahanadi Basin is affected by volcanic episodes during Early Cretaceous period (Rajmahal eruption) in both onland and shallow offshore area possibly in several phases. The synrift sediments lying beneath the volcanics are very important because of fair to good hydrocarbon potential. There are several instances where 2D seismic has failed in effectively mapping the synrift sequence mainly due to complex structural features and drastic lateral variations in the volcanics. Failure to predict the bottom of the volcanics in few wells before drilling based on 2D seismic data indicates the associated vulnerability of 2D seismic. The present study which includes both onland and shallow offshore parts of Mahanadi Basin was mainly aimed at understanding the distribution pattern of volcanics and bring out the likely distribution in virgin areas which could prove to be an invaluable aid for future exploration strategy.

A workflow was designed to estimate the depth, thickness and concentration / distribution of the volcanic episodes in hitherto less explored areas (area with sparse well data) by integrating existing 2D seismic and all other available geoscientific data. Categorisation of wells based on litho facies, thin section analysis of cutting samples, wireline log motifs and number of volcanic sills encountered was the first step. Next, structural and stratigraphic correlations along several strike and dip lines combined with isochore maps helped in the subjective analysis of areal distribution of volcanics in the study area. Subsequently, geocellular modeling approach was applied to define the complexity of the structure in terms of fault configuration to understand the flow pattern of the volcanics, probability of volcanic facies distribution, heterogeneity / spatial distribution by means of Lithofacies propagation based on kriging interpolation method using the trend modeling approach.

The present work demonstrates a unique way to conceptualise and model the distribution of volcanics in the Mahanadi Basin with available 2D seismic and other geoscientific data. Proper understanding of the distribution of volcanics by geocellular modeling approach is key for future exploration strategy in prioritising area for 3D seismic API and for identifying the most appropriate location for hydrocarbon exploration wells. The study has shown that the probability of encountering the volcanic facies is very high in areas close to the faults. The study further reveals that the presence of volcanics in the grabenal areas is quite high with shallowing up / thinning of trap over the uplifted blocks.

Introduction

Mahanadi Basin, located along the north-eastern part of East Coast of India still remains a category II basin with non-commercial discoveries of biogenic gas in the deepwater offshore. Although the Late Jurassic-Early Cretaceous petroleum system associated with the rift play presents very encouraging results in terms of rich lacustrine source rock facies encountered in well A-2 and several oil & gas indications of thermogenic origin in both onland and shallow offshore wells (viz. A-2, A-3, B-2, B-4, B-6 and B-7) (Fig. 1), discovery of any commercial field in the Basin has eluded the operators working in the basin so far. Oil India Limited (OIL) have carried out extensive exploration work in the area during the early part of the basin history with five onland wells (wells A-1 to A-5) and seven shallow offshore wells (wells B-1 to B-7) (Fig.1) but have not established any major discovery so far. The present study focuses only on the onland and shallow offshore areas of the basin. Tectonically, the Mahanadi Basin was formed during rifting and extensional breakup of the Gondwanaland during the Late Jurassic-Early Cretaceous

period. The basin was subjected to volcanism, possibly in several phases, during Early Cretaceous period (Rajmahal eruption). Earliest sedimentation in the basin started during Jurassic period followed by Cretaceous and Tertiary sedimentation. Major tectonic events are Permo-Triassic NW-SE trending fault associated with Gondwana rift, Late Jurassic - Early Cretaceous NE-SW trending rift related faults, Late Cretaceous-Recent passive margin stage. Although none of the wells drilled in the basin has encountered Gondwana sediments, but they could be expected in the deepest part of Cuttack depression, underlying the Late Jurassic-Early Cretaceous sediments.

Distribution Pattern of volcanics

While acknowledging the extreme difficulty in identifying volcanic rocks due to their complex structural features and drastic lateral variations in Subei Basin (Jiangsu Province), China, Zuo and Guozhang (2011) have brought out the typical seismic reflection characteristics and attributive characteristics to identify volcanic rocks by seismic method. In light of increasing reserves and output from volcanic rocks (Zuo and Guozhang, 2011), this trend of more research and studies on distribution of volcanic assumes much significance. In the present study, the wells were first categorised based on the formations encountered viz. Basement, Early Cretaceous and then depending on the number of volcanic sills encountered in respective wells. Based on lithological data, log motifs of typical well B-5 (Fig. 2) and thin section analysis of drill cutting sample of well A-5, three distinct volcanic sills were observed and was nomenclatured as volcanic Sill-I (V-I, top most), Volcanic Sill-II (V-II, middle) and Volcanic Sill-III (V-III, bottom most) (Fig. 2). It may be noted that the thin section analysis of well A-5 shows that the V-I consists of basalt (top section of the V-I @ 300 m) and dolerite (bottom section of V-I @ 622 m) (Figs. 4 & 5). While the thin section analysis of V-II @ 1172 m shows altered peridotite / dunite (Fig. 6). Thin section analysis for V-III section was however not carried out (Dash, 2009).

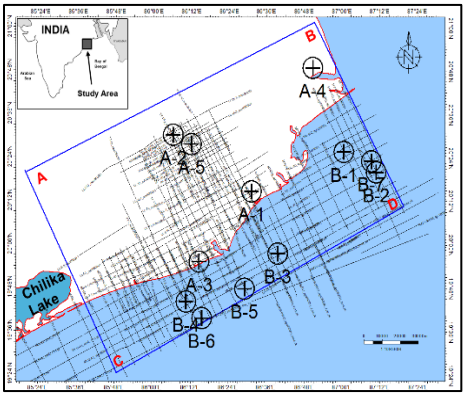

Fig. 1 Location Map showing study area (ABCD) with wells and network of 2D seismic lines.

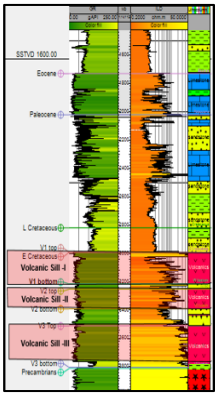

Fig. 2 Well B-5 profile.

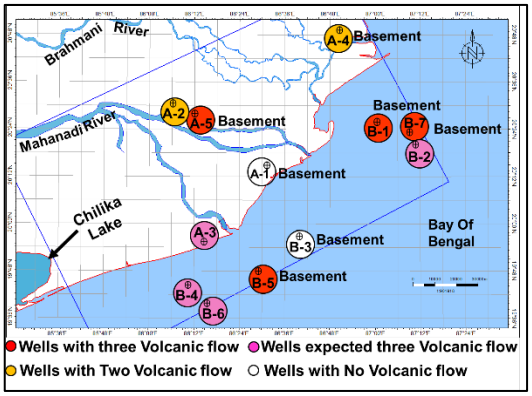

Fig. 3 Display the categorization of wells in the study area.

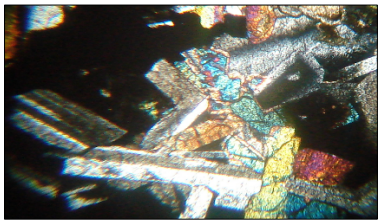

Well A-5, Depth 300 m: Basalt
Euhedral Crystals of Calcic Plagioclase (40%), Clino Pyroxene (30%) and fine grained Basaltic ground mass filling the interstitial spaces showing Ophitic texture in cross nicol position above and uncrossed position below.

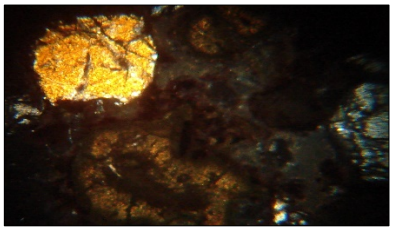

Well A-5, Depth 622 m: Dolerite/ Dunite
Olivene & Serpentinized Olivene (80-90%) with Kelyphytic border (reaction rims) and Clino-Pyroxene (10-20%) with minor Ortho-Pyroxene & Iron-Oxide rich (?) opaque mineral in cross nicol position above and uncrossed position below.

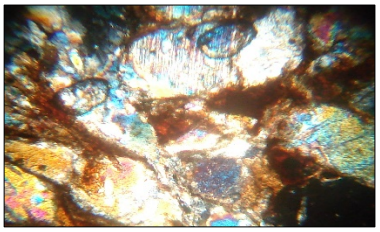

Well A-5, Depth 1172 m: Altered Peridotite/Dunite
Highly altered mostly Limonite/Goethite in background & Olivene (euhedral-subhedral grain, high relief & high birefrengence) with minor Clino-Pyroxene in cross nicol position above and uncrossed position below.

Fig. 4 photomicrograph

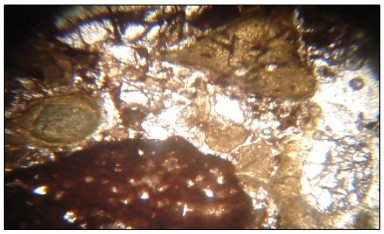

Fig. 5 photomicrograph

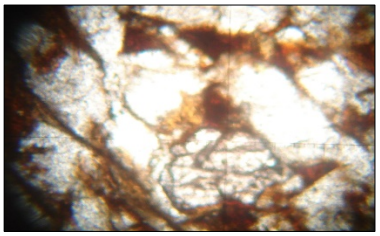

Fig. 6 photomicrograph

In the absence of isotope data or any other relevant data pertaining to age dating of the volcanic, and based on above discussed criteria of categorisation, few lithology based stratigraphic and structural correlation along dip and strike directions (NW-SE, NE-SW, E-W, N-S) were generated to understand the geometry and distribution of volcanic episodes in the study area (Figs. 9 to 13). The distribution of volcanic episodes encountered in the wells shows a typical pattern in the map view (Fig. 3). It is observed that the wells A-5, B-1, B-7 and B-5 encountered three major volcanic pulses (V-I, V-II & V-III) (Figs. 9, 10 & 12), while well A-2 encountered V-I & V-II and was terminated within Early Cretaceous period but likely presence of V-III cannot be ruled out above possible basement (Figs. 3 & 9). The well A-1 and B-3 penetrated the basement but have not witnessed any volcanic activity (Figs. 9 & 13). Fig. 7 shows the Residual Gravity Anomaly map which brings out a distinct disposition of the highs and lows corresponding to the ridges and depressions respectively. Fig. 8 shows composite seismic line passing through wells A-2, A-5 and A-1 showing the Cuttack depression, Puri depression and Nimapara-Balikuda ridge. Total absence of volcanic in A-1 & B-3 could be attributed to the likely extension of Nimapara-Balikuda ridge which might have limited the flow of volcanics (Figs 7 & 8). The well A-4 drilled in the North Eastern corner of the study area encountered V-I and V-II while V-III is absent (Fig. 10). This could probably be explained by the volcanic flow being limited due to the emerging Chandikole ridge (Fig. 7). The wells A-3, B-4 and B-2 were terminated within Early Cretaceous which penetrated the top Volcanic pulse (V-I) (Figs. 10 & 12). Correlation indicates an overall thinning and thickening of different litho-units in different horsts and grabens. The higher thickness of volcanics is generally found in the grabenal part rather than the horst part. However it may be noted that though the well A-5 is 630 m structurally updip with respect to well A-2, the higher thickness of the volcanic layer observed at A-5 could be due to the fact that the well A-5 is located on the horst block very close to the fault plane which might have acted as a conduit for the volcanics locally spilling over onto the horst block.

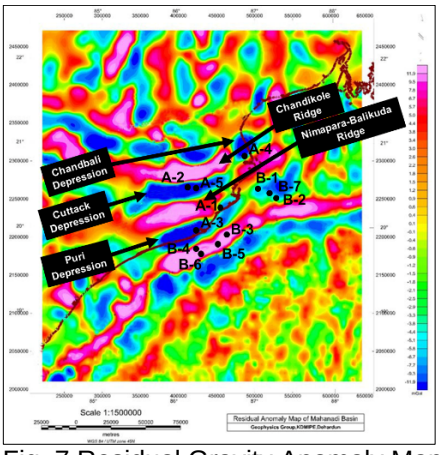

Fig. 7 Residual Gravity Anomaly Map

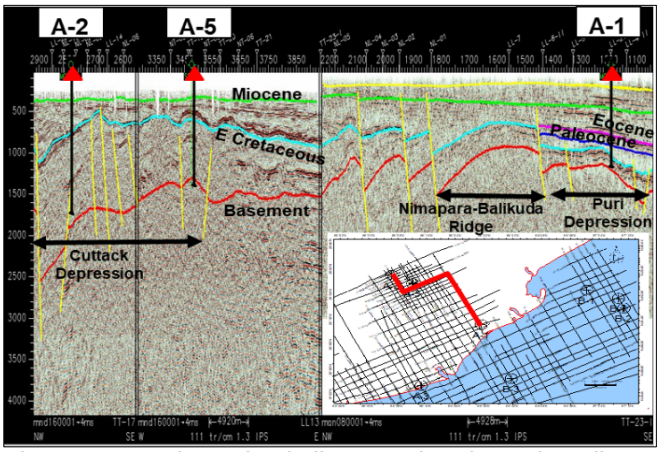

Fig. 8 Composite Seismic line passing through wells A-2, A-5 & A-1

Isochore maps (TVT) for all three volcanic episodes viz V-I, V-II and V-III were generated and they show a general trend of NNE-SSW direction. The violet colour indicates maximum thickness while the lighter turquoise colour indicates minimum thickness. Thickness map of V-I shows three major thickness trend, one towards eastern part of well A-5 with max thickness of around 660 m, second around Puri depression towards south and another trend in south-eastern part of the study area where wells B-1, B-7 and B-2 are

located (Fig. 14). This V-I trend thins out in between the areas covered by max thickness zones, apparently suggesting that the distribution of V-I episode is restricted by Nimapara-Balikuda uplift which is supported by Residual Gravity Anomaly map (Fig. 7). Remaining thickness maps for V-II and V-III almost bear the same trend but exhibits an opening up trend towards western part which could be attributed to very sparse sampling at V-II and V-III level contouring (Figs. 15 and 16).

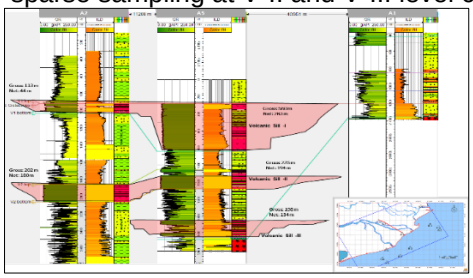

Fig. 9 Stratigraphic Correlation: A-2, A-5 and A-1 along NW-SE

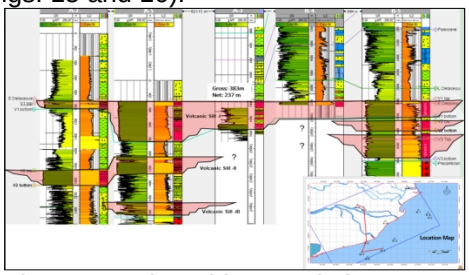

Fig. 10 Stratigraphic Correlation: A-2, A-5, A-3, B-4 and B-5 along NE-SW

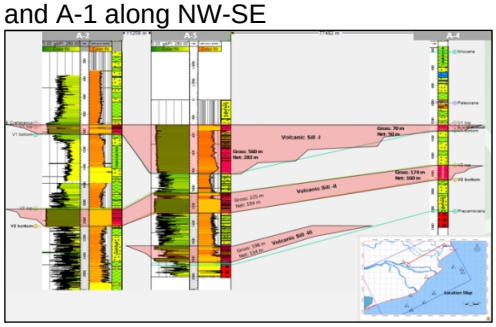

Fig. 11 Stratigraphic Correlation: A-2, A-5 and A-4 along EW

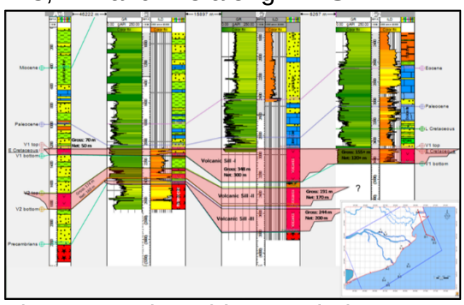

Fig. 12 Stratigraphic Correlation: A-4, B-1, B-7 and B-2 along NW-SE

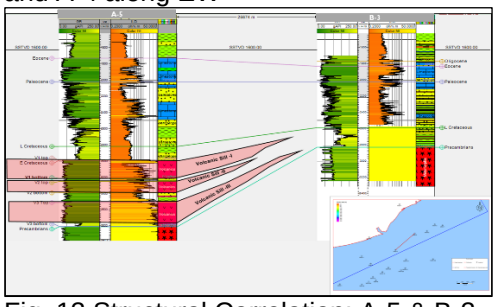

Fig. 13 Structural Correlation: A-5 & B-3 along EW

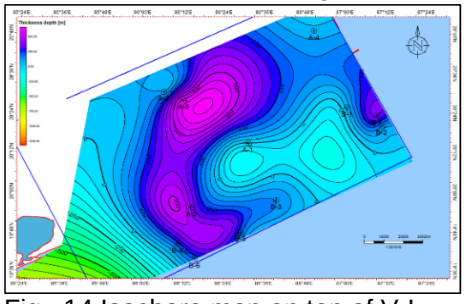

Fig. 14 Isochore map on top of V-I

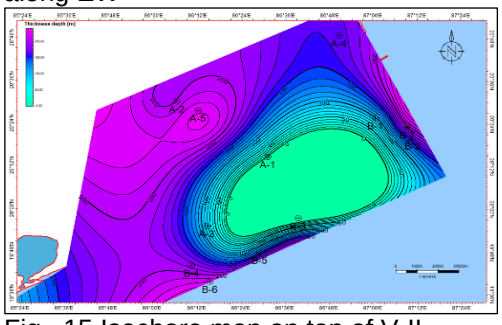

Fig. 15 Isochore map on top of V-II

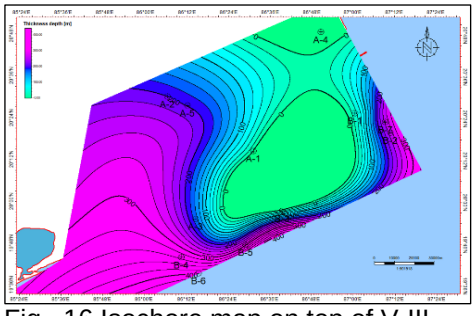

Fig. 16 Isochore map on top of V-III

Geocellular modelling approach

To strengthen the results of the above discussed conventional study, it was felt necessary to integrate the results of the conventional study with volcanic facies (V-I, V-II & V-III) propagation by means of building Geocellular model to understand the structural configuration, volcanic facies spatial distribution,

heterogeneity (Detailed workflow is presented in fig. 17). Due to data constraint, sonic logs were used to generate Time Depth Relationship. Velocity models built to convert the grid from time to depth domain for the entire onland and shallow offshore areas generated spurious and quite large anomalous difference in well tops due to data constraint particularly for the wells B-1 to B-7 lying in shallow offshore area. It was therefore decided to build two separate velocity models, one for onland and the second one for shallow offshore area to minimise the mistie differences. The Fault pattern map shows two major fault trends, the dominant fault trend is defined by ENE-WSW to NE-SW trending faults that have shaped the horst and graben topography in the synrift sequence. Faults are extensional normal faults. A total of 13 faults (F1 to F13) in onland area and 6 faults (F14 to F19) in Shallow offshore area were interpreted. The structural framework for the model has been constrained by the seismically interpreted horizons for Early Cretaceous and Basement level, fault interpretation from 2D seismic data and honouring all well data. Structure model was built in depth domain, constrained by the 2D seismic interpretation results and well data. The grid cell size was taken equal to 1500mX1500mX50m because of the large area included in this model in both the cases. In order to derive maximum information about the distribution of the volcanics in the area and its behaviour, a process called 'zoning' (V-I, V-II & V-III) has been introduced within the sequence bounded by two surfaces namely Early Cretaceous and Basement. Same workflow was used for both the onland and shallow offshore model. A simple petrophysical interpretation method utilised for this study helped relatively accurately the identification of volcanic facies in spite of wireline log constraints. Petrophysical rock types were characterized based on log calculation from Gamma ray, Resistivity & Porosity values. With the input of cut off values, reasonable rock typing for volcanic rocks and a good correlation between the discrete lithology log, electrical log and facies log generated using the cut off values could be established (Fig. 18). Rock typing based on cut off value for volcanic rock is GR<=70, ILD>=10, NPHI<=0.09.

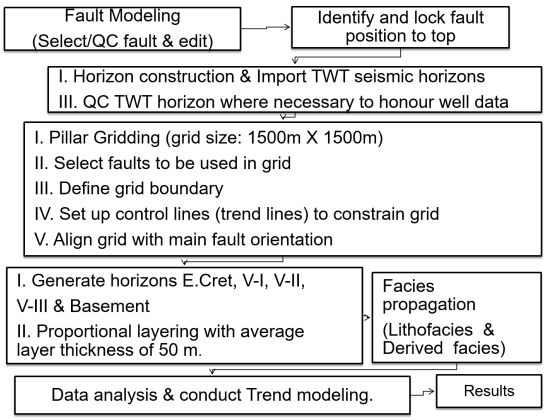

Fig. 17 Geomodeling Workflow

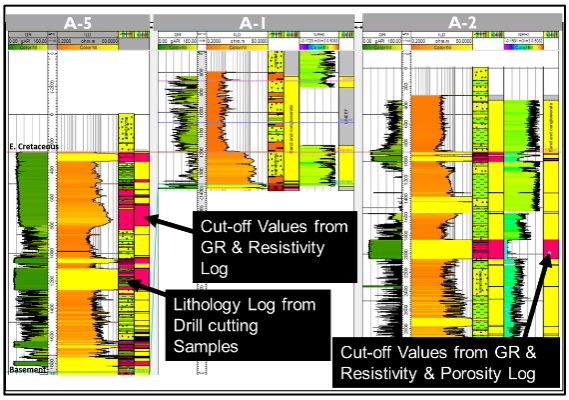

Fig. 18 Comparative display: Electric log, Lithology log and facies log (based on cut off value)

Variogram analysis was performed for each facies to estimate the trends correlation and a general trend of NE-SW direction was given within Early Cretaceous zone based on tectonic map with a search radius of 50-60 km and 20 km in major and minor direction respectively. Data analysis was performed for each facies so that the well data correctly represent the property's distribution to match the interpretation of the volcanic facies distribution. Histograms for the zone and facies of the model was reviewed to ensure that the model is reasonable, represents the data, and matches geologic interpretation. 3D probability volumes for each facies within Early Cretaceous zone through kriging interpolation and block averaging for litho facies and derived facies based on cut-off values were generated. Discrete trend modelling is based on block kriging of the probabilities of each of the facies to create vertical proportion volumes. Objective of this trend model is primarily to understand spatial distribution of volcanic rocks in the study area. In order to predict volcanic facies distribution away from the well, a number of property attribute maps were generated from the 3D grid for both onland and shallow offshore areas. The three key surfaces V-I, V-II and V-III ascribed to three volcanic sills were considered most likely to yield information on the behaviour of distribution pattern of volcanics. The V-I exhibits NNE-SSW trend and is well developed in the SW direction with 60% - 65% probability, whereas the same is thinned out towards the well A-2 in the grabenal part along NNW direction with probability of 30% to 40% (Fig. 19). This

observation assumes significance because the area close to the northern half graben bounding fault of Cuttack depression, where a sedimentary column of 5 km is expected, becomes promising from hydrocarbon prospectivity point of view. Maximum probability of occurrence is observed towards SSW of well A-5. The trend continues towards the Puri-Konark Depression along SSW direction towards well A-3. The V-I probability is less in area encircling the well A-1 in Puri depression. The trend map of V-I generated from the derived facies model also shows the similar trend with that of litho facies trend (Fig. 20). The V-II probability appears to be high in the area NE and SE of A-5. The lateral continuity is sporadic and fades away further SSW direction (Figs. 21 & 22). The V-III probability is high in and around both the wells A-5 and A-2 and it appears that the first volcanic eruption filled the pre-existing deeper grabenal parts in Cuttack depressions with a probability of 60% towards North (Fig. 23). The probability of encountering the volcanic facies is very high in areas close to the faults which played a key role in eruption of Volcanics through fissures in the crust. Similarly the trend for the derived facies is similar but the probabilities are slightly higher in magnitude which could again be attributed to the uncertainty caused by data constraint due to lack of electrical logs (Fig. 24). Similar methodology was adopted for Shallow Offshore area also. Distribution of volcanic is observed to be relatively more in concentration in the SSW of well B-5. In and around the wells B-1, B-7 and B-2 in NNE direction, the probability of encountering volcanics is 80% to 90%, whereas the same is perhaps thinned out towards the well B-3 with probability of 0% (Fig. 25). Max probability of occurrence is observed towards the NNW direction with reference to well B-5 in all levels (Figs. 25, 27 & 29). It appears that the maximum probability trend continues towards the Puri Depression towards well A-3 in onland area. Similarly probability trend for the derived facies observed reasonable match (Figs. 26, 28 & 30).

Probability Maps: Lithofacies Vs Derived Facies for onland area

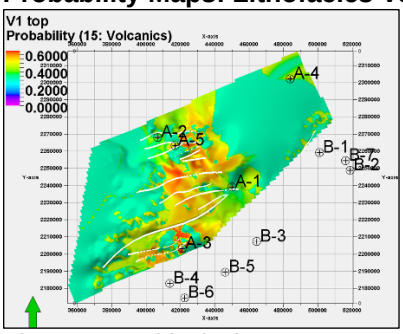

Fig. 19 V-I: Lithofacies

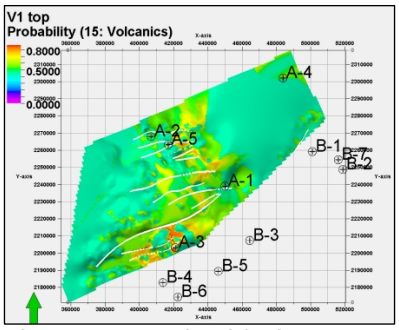

Fig. 20 V-I: Derived facies

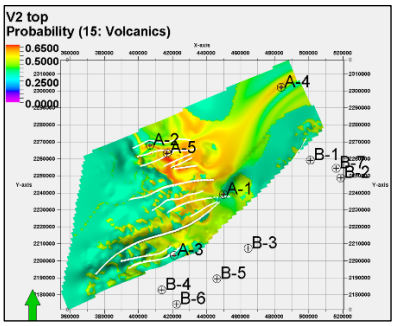

Fig. 21 V-II: Lithofacies

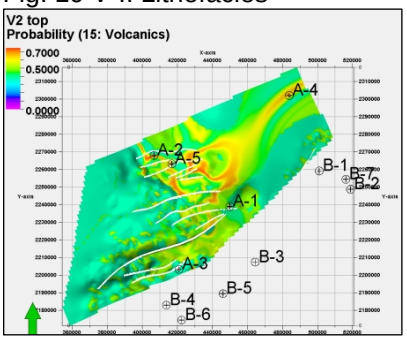

Fig. 22 V-II: Derived facies

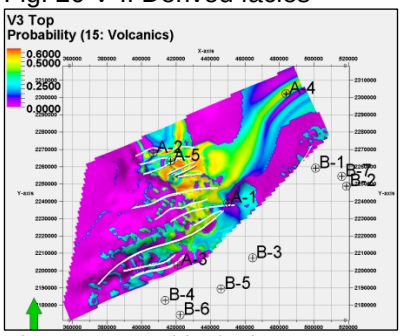

Fig. 23 V-III: Lithofacies

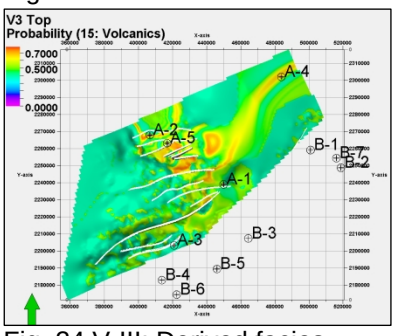

Fig. 24 V-III: Derived facies

Probability Maps: Lithofacies Vs Derived Facies for shallow offshore area

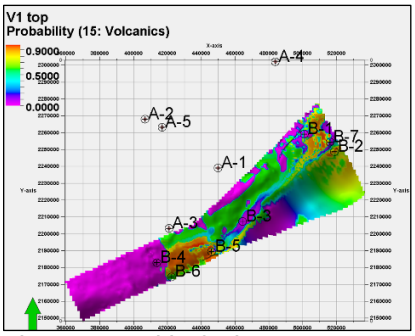

Fig. 25 V-I: Lithofacies

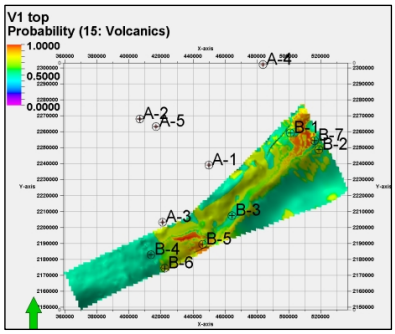

Fig. 26 V-I: Derived facies

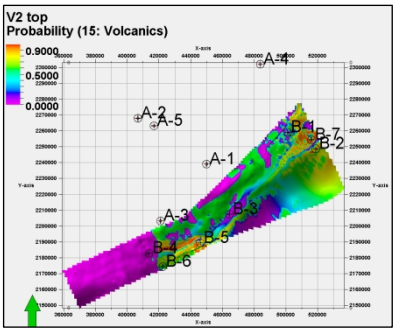

Fig. 27 V-II: Lithofacies

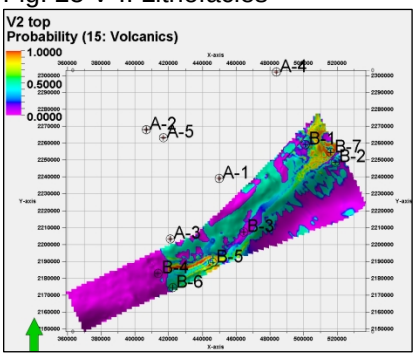

Fig. 28 V-II: Derived facies

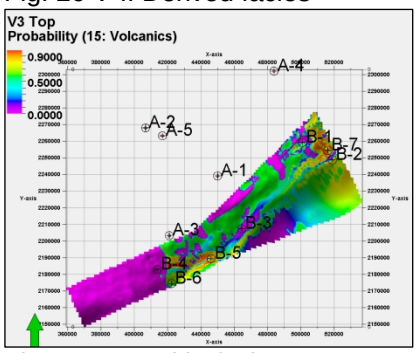

Fig. 29 V-III: Lithofacies

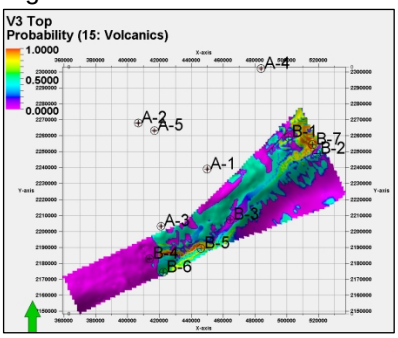

Fig. 30 V-III: Derived facies

Conclusion

Lateral variations in distribution of volcanics in the onland and shallow offshore Mahanadi Basin at different phases within Early Cretaceous period assumes significance in light of the increasing reserves and output from volcanic rocks in few sedimentary basins worldwide. The present work demonstrates a unique way to conceptualise and model the distribution of volcanics in the Mahanadi Basin with available 2D seismic and other geoscientific data through geocellular modelling approach. Results thus obtained could be integrated in the future with 3D seismic and geo-statistical modeling to have a more robust deterministic approach to aid in hydrocarbon exploration. Proper understanding of the distribution of volcanics is key for future exploration strategy in prioritising choice of area for 3D seismic and later for choosing the best location for hydrocarbon exploration wells. The study has shown that the probability of encountering the volcanic facies is very high in areas close to the faults. The study further reveals that the presence of volcanics in the grabenal areas is quite high with shallowing up / thinning of trap over the uplifted blocks. The probability of maximum thickness of V-I is around 10 km NNW of well A-3. Similarly, V-II is expected with highest probability at around 20 km ESE from well A-5 and V-III at around 18 km SE of well A-5. In the shallow offshore, maximum probability for all the volcanic episodes is predicted to be around 12 km in ENE direction from well B-4. It is however, recommended to have a detailed mineralogical / petrophysical modeling in order to understand the precise facies variations using state of the art mineralogical tools in future studies.

Acknowledgement

The authors express their sincere gratitude to Shri. A.K. Dwivedi, Director (Exploration), ONGC and Dr. P. Chandrasekaran, Director (E&D), OIL for their permission to publish this paper. The authors are very much thankful to Shri S. K. Jena, ED (E&D)-Corporate, Shri Swadesh Dey, ED (KGB & BEP) and Shri B. R. Bharali GM (Geosciences) OIL for their valuable guidance in preparation of this paper. Thanks are due to Shri S. K. Das, GGM-MBA Basin, ONGC and Shri B. N. Pradhan, DGM (GP)-Head, ONGC, for their encouragement and providing guidance and help.

References

Dash D, 2009, A Note on Basement as encountered in the Well A-5, OIL Unpublished report.

Zuo G and Guozhang Fan, 2011, A Study of Volcanic Rocks Identification by Seismic Methods in Subei Basin, Jiangsu Province, China, AAPG Annual Convention and Exhibition, Houston, Texas, USA.